

Cite this: *Soft Matter*, 2012, **8**, 6620

www.rsc.org/softmatter

PAPER

## Tuning suspension rheology using capillary forces

Erin Koos,<sup>\*</sup> Julia Johansmeier,<sup>†</sup> Linda Schwebler,<sup>‡</sup> and Norbert Willenbacher

Received 24th March 2012, Accepted 26th April 2012

DOI: 10.1039/c2sm25681a

When a small amount (less than 1%) of a second immiscible liquid is added to the continuous phase of a suspension, the rheological properties of the admixture are dramatically altered and it can change from a fluid-like to a gel-like state. The rheological properties can be modified through changes in the particle size, temperature induced changes to the interfacial tension, and through the addition of surfactants. These changes are experimentally investigated in this current work, concentrating on the capillary (non-wetting) state with additional experiments in the pendular (wetting) state. The yield stress scales with the interfacial tension and reciprocal radius ( $\Gamma/r$ ) as expected due to the capillary nature of the attractive force leading to network formation and gelation. The addition of surfactants leads to a drastic reduction in the yield stress and viscosity, which is attributed to a partial trapping of the secondary fluid within surfactant micelles.

### Introduction

Capillary suspensions, suspensions with a small amount of a second immiscible liquid, have a broad spectrum of potential applications.<sup>1,2</sup> In these suspensions, the addition of a secondary fluid either reinforces an existing space-spanning network created by, *e.g.*, the van der Waals force or can even create a network when the particles are well stabilized.<sup>3–5</sup> Capillary suspensions can be used to suspend hydrophilic particles in hydrophobic liquids (and *vice versa*) without the modification of particle surface properties and can prevent the settling of particles. The phenomenon can be used to adjust the flow properties of coatings, adhesives or other complex fluids according to the requirements in particular processing steps and may even be used to create low-fat food products with appropriate texture. The capillary force usually dominates over other colloidal forces.<sup>6</sup> The strong network found in these suspensions even persists when the major fluid is removed and thus provides a new pathway for the creation of microporous membranes, foams and ceramics with unprecedented high porosity at small pore sizes.<sup>7</sup>

Depending on the wetting angle of the secondary fluid, two distinct states are defined. In the pendular state, the secondary fluid preferentially wets the particles and a meniscus forms between particles. The particle–fluid admixture is in the capillary state when the secondary fluid does not preferentially wet the particles. In the pendular state, a sample-spanning network is composed of particles linked by capillary bridges.<sup>1,8</sup> In the

capillary state, the network consists of clusters of particles around small volumes of the secondary fluid.<sup>9</sup> Previous investigations have shown that capillary suspensions can undergo a transition to a gel-like state at volume fractions as low as  $\phi = 0.10$ —well below the limit of dense packing—increasing the yield stress and viscosity by several orders of magnitude as the volume fraction of the second fluid is increased.<sup>1</sup>

Both the capillary state and pendular state are controlled by the capillary force and are strongly influenced by changes in the amount of secondary fluid and the material properties. In air, the force between two particles depends on the particle radii, the surface tension  $\Gamma$  of the fluid spanning the particles, and the wetting angle  $\theta$  that the fluid makes with the solid surface. The force between two equally-sized spheres of radius  $r$  connected by a pendular bridge is given by,

$$F_c = 2\pi r \Gamma \cos\theta, \quad (1)$$

where it is assumed that the particles are in contact and that the pendular bridge is small with respect to the radius of the particles. For larger droplets, the force will depend on the volume of the secondary fluid, with various corrections given based on the filling angle and shape of the droplet.<sup>10–13</sup> Additional corrections are available for particles that are not in contact or include surface roughness.<sup>14–17</sup> The resulting yield stress for a macroscopic sample of such bridged particles (wet granular media) is

$$\sigma_y = f(\phi)g(\tilde{V})\frac{\Gamma\cos\theta}{r}, \quad (2)$$

where  $f(\phi)$  is a function of the volume fraction of particles within this sample and  $g(\tilde{V})$  is a function of the normalized droplet volume  $\tilde{V} = V/r^3$ .<sup>18,19</sup> This function  $g(\tilde{V})$  has a maximum value of unity when the droplets are neither under nor overfilled.<sup>10,13</sup> The particle loading, packing geometry, and the number of

Institute for Mechanical Process Engineering and Mechanics, Karlsruhe Institute of Technology, Gotthard-Franz-Straße 3, Bldg. 50.31, 76131 Karlsruhe, Germany. E-mail: erin.koos@kit.edu

<sup>†</sup> Present address: University of Hohenheim, Garbenstraße 25, 70599 Stuttgart, Germany.

<sup>‡</sup> Present address: BASF SE, Process Research and Chemical Engineering, GCP/TR – L549, 67056 Ludwigshafen, Germany.

particle–particle contacts each influence  $f(\phi)$ , but for sparse mixtures,  $f(\phi) = \phi^{2.19}$

In capillary suspensions, the particles are suspended in a bulk fluid rather than in air. The particles are connected by bridges of the secondary fluid in the pendular state, analogous to wet granular media, but here, the force is proportional to the interfacial tension  $\Gamma_{SB}$  and the principle wetting angle is the two-fluid contact angle  $\theta_{S,B}$  that the secondary fluid makes with the solid particles while surrounded by the bulk fluid. In a previous article, we used a computational model to examine particles surrounding small droplets of secondary liquid in the capillary state.<sup>9</sup> These particle subgroupings can arrange in tetrahedral, octahedral, or higher order structures depending on the secondary fluid content and the contact angle that the secondary fluid makes with the solid particles. When the contact angle becomes high, certain particle arrangements become inaccessible (*e.g.* greater than  $151.2^\circ$  for tetrahedral and  $165.3^\circ$  for octahedral structures). These clusters form the basic building blocks of the space-spanning network in the capillary state and the rheological features these suspensions can be nicely rationalized on the basis of this cluster model. For these suspensions, the  $\cos\theta$  in eqn (2) has to be replaced by another function of the two-fluid contact angle, which is not yet known. The dependence on the interfacial tension and reciprocal radius will remain in place for capillary state suspensions. Any of the material parameters given in eqn (2) can be used to tune not only the yield stress, but also the other rheological properties of the capillary suspensions.

The present paper is meant to continue our previous work describing capillary suspensions<sup>1</sup> and the cause of gelation when the secondary fluid does not preferentially wet the particles.<sup>9</sup> This paper looks at how the strength of capillary suspensions can be adjusted through the choice of particle size, the addition of surfactants, or changes to the interfacial tension, which is tuned here by variations in the sample temperature. The next section describes the sample preparation and experimental procedures. The results and analysis are described in the following section.

## Experimental methods

### Sample preparation

Experiments were conducted using two different particle systems: glass and hydrophobically modified calcium carbonate. The calcium carbonate particles were manufactured by Solvay Advanced Functional Minerals (Socal U1S1, Salin de Giraud, France). The glass, obtained from Potters Europe (Spherglass 3000 and 5000 Solid Glass Microspheres, Kirchheimbolanden, Germany), was sieved to create the desired particle size distributions. (Images of the particles used in this paper may be found in the supplementary online information of our previous work.<sup>1</sup>) The particle sizes were measured using LALLS (Low Angle Laser Light Scattering, Sympatec HELOS H0309) when suspended in ethanol and subjected to ultrasonic dispersion. (The particles were suspended using a Sympatec QUIXEL unit.) The hydrophobic calcium carbonate particles have an average radius of  $0.79\ \mu\text{m}$ . The glass particles have radii ranging between  $1.19\ \mu\text{m}$  and  $18.5\ \mu\text{m}$ , as shown in Fig. 1.

The samples used throughout this paper were created using thoroughly dried particles (dried overnight at  $70\ ^\circ\text{C}$ ), which

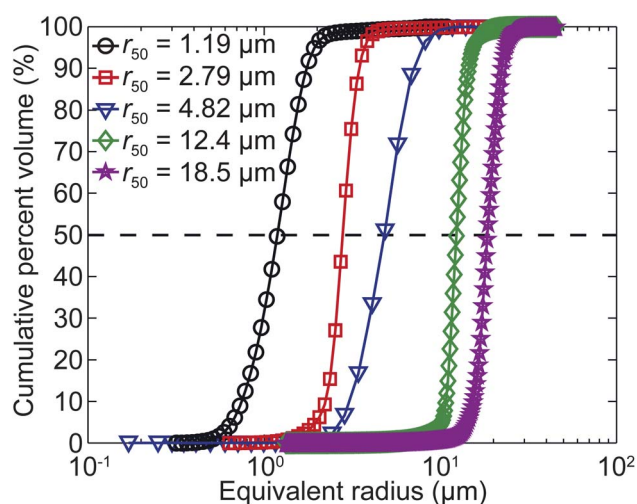


**Fig. 1** The cumulative percent volume for the glass particles used in this study. Each size range of particles has a unimodal distribution with the average radii ranging between  $1.19\ \mu\text{m}$  and  $18.5\ \mu\text{m}$ .

were suspended in either silicone oil (AK200, Wacker Chemie AG, Burghausen, Germany) or diisononyl phthalate (DINP, Henkel AG, Düsseldorf, Germany) with added water. The silicone oil and DINP have viscosities of  $190\ \text{mPa}\ \text{s}$  and  $78\ \text{mPa}\ \text{s}$  at  $20\ ^\circ\text{C}$ , respectively. The particles were mixed into the bulk fluid using a turbulent beater blade until a uniform suspension was created (at  $500\text{--}2000\ \text{rpm}$  for  $20\ \text{min}$ ). This mixture was again dried overnight at  $70\ ^\circ\text{C}$  to remove any water that may have condensed during mixing and was held under vacuum ( $100\ \text{mbar}$ ) to remove air bubbles. At room temperature, the secondary fluid was added to the suspension and thoroughly mixed using a propeller stirrer (at  $500\text{--}1000\ \text{rpm}$  for  $10\ \text{min}$ ). The samples were held in air-tight containers until the measurements were completed.

The capillary suspensions are characterized using the saturation of the preferentially wetting fluid  $S$ ,

$$S = \frac{V_{\text{wetting fluid}}}{V_{\text{total fluid}}}, \quad (3)$$

which is close to zero for the pendular state and approaches one for the capillary state.<sup>20,21</sup> The admixtures are also characterized by the two-fluid wetting angles, which are calculated from the wetting angles that the fluids make with respect to the particles in air. The fluid wetting angles were determined using a modified Washburn method for the capillary rise of a fluid through a dry powder in air<sup>22</sup> using a DataPhysics DCAT 21 tensiometer (Filderstadt, Germany). For fluid–particle combinations with contact angles greater than  $90^\circ$  in air, *i.e.*, hydrophobic particles in water, particles were attached to a Wilhelmy plate using double-sided tape and the advancing contact angle was measured.<sup>23</sup> These values were adjusted to account for errors due to surface roughness following the method of Yan *et al.*<sup>24–26</sup> Using these wetting angles and the material properties, the two-liquid wetting angle is calculated using the Young equation<sup>27,28</sup> as

$$\cos\theta_{S,B} = \frac{\Gamma_{S_a}\cos\theta_{S,a} - \Gamma_{B_a}\cos\theta_{B,a}}{\Gamma_{SB}}, \quad (4)$$

where the subscript  $a$  refers to air,  $B$  the primary (bulk) liquid, and  $S$  the secondary liquid. The wetting angle  $\theta_{i,j}$  is the angle fluid  $i$  makes against the solid in an environment provided by fluid  $j$ . The interfacial tension  $\Gamma_{ij}$  is measured at an interface between fluid  $i$  and fluid  $j$ , as was measured using a Wilhelmy plate on the same tensiometer. The dependence of the product  $|\Gamma_{SB} \cos\theta_{S,B}|$  on temperature is shown in Fig. 2.

To investigate the influence of surfactants on capillary suspensions, three nonionic surfactants and one ionic surfactant were tested. These surfactants were chosen for their differing hydrophilic–lipophilic balance (HLB), which describes the suitability of the surfactants for various applications. The nonionic surfactants were polyoxyethylene (20) sorbitan monolaurate (Tween 20, HLB = 16.7), polyoxyethylene (20) sorbitan trioleate (Tween 85, HLB = 11.0) and sorbitan monooleate (Span 80, HLB = 4.3). In addition to the nonionic surfactants, the ionic surfactant dioctyl sulfosuccinate sodium salt (DOSS, HLB = 10.9) was also used. The surfactants were obtained from Sigma-Aldrich and the nonionic surfactants were dried overnight at 70 °C to remove moisture prior to use. The ionic surfactant was used as supplied. Samples containing these surfactants were prepared as described above with the surfactant added at the same time as the secondary fluid (water).<sup>29</sup>

The interfacial tension between water and silicone oil without surfactant is 39.8 mN m<sup>-1</sup>. The addition of small amounts (>1 mM) of nonionic surfactant significantly reduces the interfacial tension to 5.7 mN m<sup>-1</sup>. This behavior is typical for concentrations well above the critical micelle concentration (CMC  $\approx 10^{-2}$  mM for the surfactants used here).<sup>30,31</sup> The effect of the ionic surfactant on the interfacial tension is similar to those of the nonionic surfactants with the interfacial tension dropping to an average value of 3.5 mN m<sup>-1</sup> with surfactant.

### Experimental procedure

The strength of capillary suspensions is primarily measured through the yield stress. These measurements were conducted using a con-plate rheometer (RheoScope 1, Thermo Fisher

Scientific, Karlsruhe, Germany). The yield stress is defined as the stress at which the sample begins to deform plastically. These measurements were conducted using a stress-ramp, where the yield stress was found as the point at which the slope of the logarithmic deformation (as a function of the logarithmic shear stress) changes from a very low (nonzero) value to a high value. Further confirmation of yield was provided by a drastic reduction in the measured viscosity. These points were evaluated using the RheoWin software and a Matlab algorithm. The shear stress ramp was conducted over 20 min starting at least two orders of magnitude below the yield stress and ending at least an order of magnitude higher than the yield stress, which minimized the error between the samples.<sup>32</sup> Experiments were repeated several times to ensure that the ramp limits were sufficient and that the experimental values were consistent.

In addition to yield stress measurements, the sample viscosity was measured using a shear rate step. The shear rate was increased incrementally and held at a constant value, for at least 30 s and for a maximum of 120 s, until the stress reached a steady state,  $(\Delta\sigma/\sigma)/\Delta t < 0.01\% \text{ s}^{-1}$ , before recording the shear stress and corresponding viscosity. These experimental procedures are identical to and described in more detail in previously published measurements of capillary suspensions.<sup>1,2,9</sup>

## Results and discussion

The strength of capillary suspensions can be altered by changing the interfacial tension, particle size or with the addition of surfactants. These influences are discussed in the following sections.

### Interfacial tension

Interfacial tension can be tuned by the variation of the sample temperature. The interfacial tension will decrease with increasing temperature for the majority of fluid combinations and temperature ranges.<sup>33–35</sup> The influence of the interfacial tension was investigated using samples prepared using hydrophobic calcium carbonate suspended in silicone oil (AK200,  $\phi = 0.11$ ) with added water (capillary state,  $\theta = 139.2^\circ$ ). The typical normalized yield stress for the capillary suspensions is shown in Fig. 3a, where the sample temperature for this capillary state suspension was varied between 10 °C and 60 °C. For the yield stress, normalized by the samples without added water, all of the curves show a typical shape with very little increase in the yield stress at low secondary fluid concentrations (larger fractions of wetting liquid), a drastic increase in yield stress and then a slow-growth or plateau region at larger added secondary fluid concentrations (smaller fractions of wetting liquid). For this particle–liquid combination, the yield stress increases by more than two orders of magnitude with the addition of 0.5% added water corresponding to a saturation  $S = 0.994$ .

The normalized yield stress curves (Fig. 3a) vary with the sample temperature. There was very little deviation between the plateau yield stress for experiments conducted at 40 °C and 60 °C, but there were significant differences at other temperatures. Reducing the sample temperature resulted in

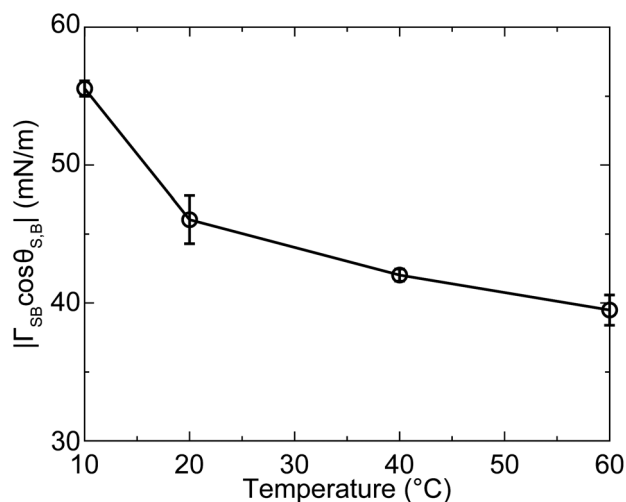
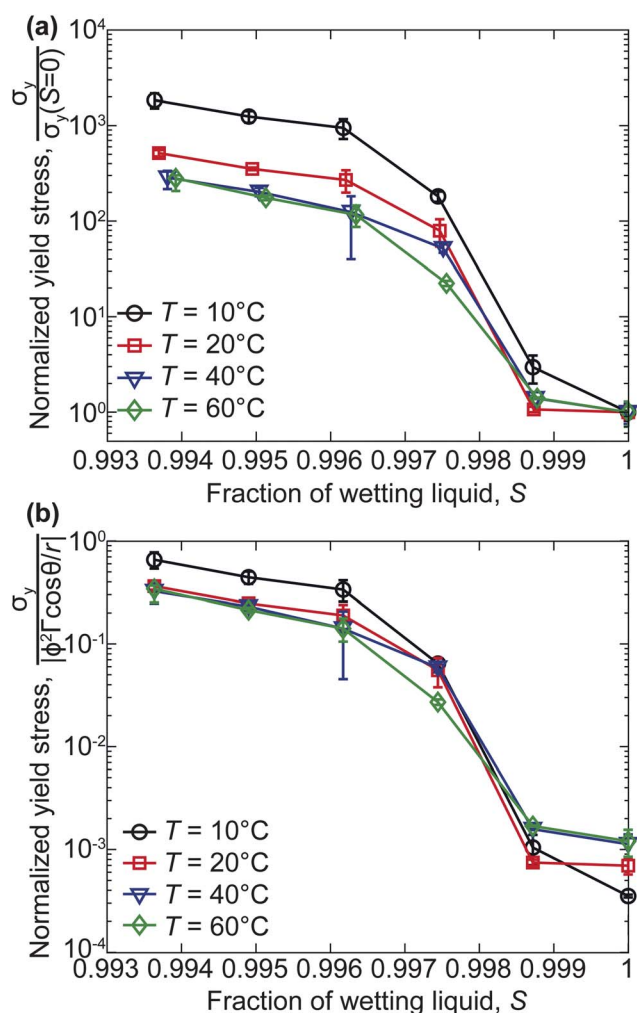


Fig. 2 Influence of sample temperature on interfacial energy  $|\Gamma_{SB} \cos\theta_{S,B}|$ . (Hydrophobic calcium carbonate,  $r = 0.79 \mu\text{m}$ , in silicone oil with added water.)



**Fig. 3** (a) The yield stress at four different temperatures normalized by the yield stress with no added water. (b) The yield stress normalized by the predicted capillary strength ( $|\phi^2 \Gamma \cos \theta / r|$ )<sup>36</sup> to eliminate the influence of temperature on the strength of the samples. (Hydrophobic calcium carbonate,  $r = 0.79 \mu\text{m}$ , in silicone oil at  $\phi = 0.11$  with added water, capillary state.)

a corresponding increase in the measured yield stress with a slight increase at  $20^\circ\text{C}$  and an even greater increase in the yield stress at  $10^\circ\text{C}$ , where the interfacial tension is the largest.

We normalized the calculated yield stress by the capillary stress (eqn (2)), and additionally the effect of the particle size and volume fraction is included, where  $f(\phi)$  is given by  $\phi^2$  for sparse mixtures.<sup>19</sup> Then, the yield stress curves begin to collapse onto one master curve as shown in Fig. 3b. The yield stress curve for the lowest temperature,  $10^\circ\text{C}$ , is slightly higher than for the other temperatures either due to an error in the measurement of  $|\Gamma \cos \theta|$  or in the predicted dependence on these parameters. These curves also plateau towards the value of  $\sigma_y = |\phi^2 \Gamma \cos \theta / r|$ , the maximum strength that a network formed by a sparse volume fraction of particles connected by capillary bridges can obtain. While this mixture is in the capillary state and forms clusters rather than individual particles connected by a capillary bridge, the maximum strength should approximately correspond to this value.

Typical flow curves both with and without added secondary liquid are shown in Fig. 4. Capillary suspensions are shear thinning—the viscosity decreases with increasing shear rates—and the admixtures with secondary fluid approach the same viscosity as samples without added water at the highest shear rates. Without added water (open symbols), the viscosity is shear thinning and there is a slight variation with temperature. At low shear rates, increasing temperature increases the viscosity. At high shear rates, there is a reduction of the viscosity with increasing temperature. The strong shear thinning of the suspensions without added water indicates attractive vdW interactions among particles and the formation of a sample-spanning network structure. At high shear rates, the network breaks up into aggregates, but the viscosity is still about three times higher than expected for a hard sphere suspension with  $\phi = 0.11$ . According to Batchelor<sup>37</sup> such a suspension is expected to have a viscosity  $\eta = 330 \text{ mPa s}$  at  $20^\circ\text{C}$  when pairwise hydrodynamic interactions are taken into account. The significantly higher viscosity obtained here clearly indicates the existence of flocs immobilizing part of the solvent with the floc size seeming to be temperature dependent. Shear thickening occurs in the investigated shear rate range at  $10^\circ\text{C}$  and  $20^\circ\text{C}$ . The critical shear rate for the onset of thickening corresponds to a floc radius of about  $2 \mu\text{m}$ , which is slightly more than twice the particle radius.<sup>38</sup>

With added water, the effect of the temperature variations on the admixture viscosity is more dramatic. Increasing the sample temperature decreases the measured viscosity at all shear rates. The greatest change in the viscosity is at  $60^\circ\text{C}$  with only a slight difference in the viscosity between the  $40^\circ\text{C}$  sample and the lower temperature samples. There is no apparent difference between the viscosity at  $10^\circ\text{C}$  and  $20^\circ\text{C}$ . The changes to the admixture viscosity mirror the changes in the bulk fluid viscosity with the exception of the highest temperature sample at low shear rates. For this sample, the viscosity is reduced by

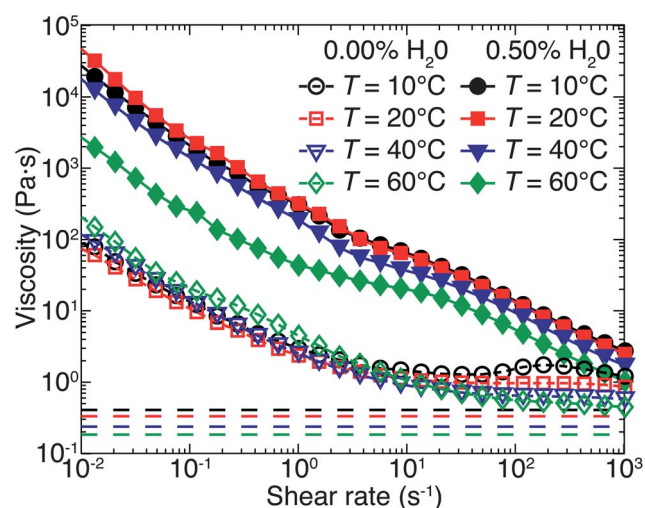


**Fig. 4** Flow curve without and with 0.5% added water as a function of temperature. The lower dashed lines give the effective viscosity for a hard sphere suspension using the relation of Batchelor.<sup>37</sup> (Hydrophobic calcium carbonate,  $r = 0.79 \mu\text{m}$ , in silicone oil,  $\phi = 0.11$ , with added water, capillary state.)

an order of magnitude from the other samples—much greater than the change to the bulk fluid viscosity. This temperature data also shows a slight plateau, where the shear thinning behavior becomes less pronounced at intermediate shear rates ( $10^0$ – $10^1$  s $^{-1}$ ).

The much higher low shear viscosity of the suspensions with added water reflects the formation of a strong network controlled by capillary forces. This network breaks up when exposed to a shear field, but even at the highest applied shear rates, the viscosity remains higher than for the samples without added water. The strong capillary force continues to cause some agglomeration immobilizing more of the solvent than in the case without added water. As the shear rate increases past the measured values, the clusters agglomerated through the capillary force will presumably continue to break up and the viscosity curve is expected to merge with the values without added water.

These mixtures are also completely reversible when the secondary fluid content is evaporated. The yield stress for  $\phi = 0.11$  CaCO $_3$  in silicone oil increased from 0.5 Pa to 250 Pa with 1% added water. Such a sample was placed in an oven at 100 °C for several days and periodically stirred or shaken to hasten the evaporation of the water. Following this procedure, the sample returned to its original state with a much lower yield stress and viscosity. The yield stress of the evaporated sample was then compared with an original sample where no secondary fluid was added. These two samples exhibited the same yield stresses within experimental error. This evaporation process was repeated several times with no apparent degradation of the sample.

### Particle size

The force between two particles connected by a capillary bridge is proportional to the particle size. The stress, however, is proportional to the reciprocal radius due to the influence of the area of force contact.<sup>20</sup> The yield stress of a capillary suspension will depend on the reciprocal radius of the particles used, such that the strength of the suspension increases as the radius is decreased. This was confirmed using clean glass beads suspended in DINP ( $\phi = 0.30$ ) with added water (pendular state,  $\theta = 49.4^\circ$ ). This dependence is most easily appreciated through the different consistencies of the materials, as displayed in the images of Fig. 5. The shear stress associated with a sample of particles joined by pendular bridges, as described in eqn (2),

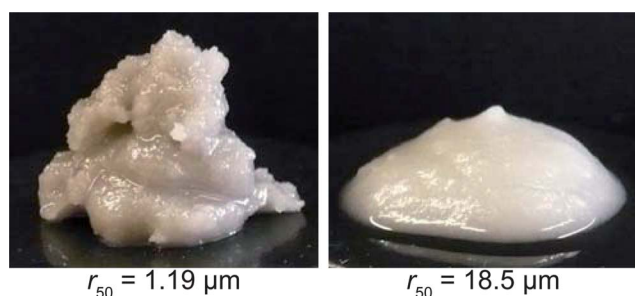


**Fig. 5** Sample images with  $r = 1.19$   $\mu\text{m}$  and  $r = 18.5$   $\mu\text{m}$  sized particles, both with 0.60% added water. (Clean glass,  $\phi = 0.30$ , in DINP with added water, pendular state.)

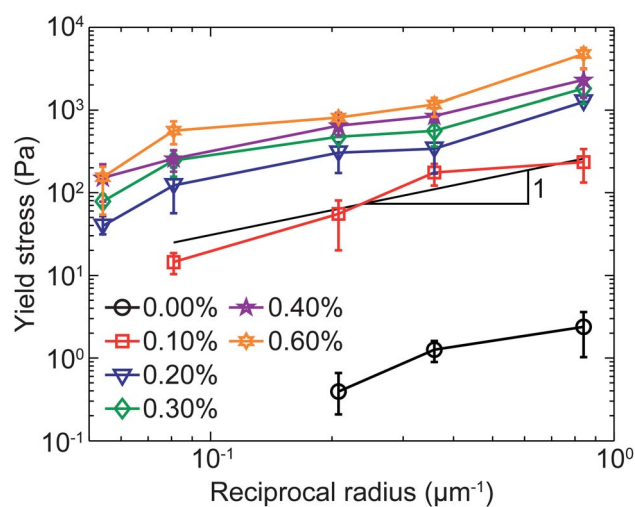


**Fig. 6** Yield stress as a function of the particle reciprocal radius in the pendular state. (Clean glass,  $\phi = 0.30$ , in DINP with added water, pendular state.)

should vary linearly with the reciprocal radius of the particles. The yield stress (Fig. 6) follows this linear dependence for almost every fraction of the added water and every particle size tested. The strength of a capillary space-spanning network is greater for smaller particles than for larger particles. This difference is readily apparent in the missing points in Fig. 6; for these mixtures, the cohesion between particles is insufficient to prevent phase separation.

The dependence of the capillary suspension viscosity on particle size is slightly more complicated. The measured viscosity curves are shown in Fig. 7a both without and with 0.6% wt. secondary liquid. The two pure suspensions with the larger particles are almost Newtonian fluids with viscosities close to the value predicted using the relation of Quemada,<sup>39</sup> where  $\phi_m = 0.6$ . The viscosity for the pure suspensions using the smaller sized particles is larger than the predicted viscosity at low shear rates due to the vdW attraction, but decreases towards the theoretical value for hard sphere suspensions at higher shear rates. For the mixtures with added secondary fluid, the viscosity is significantly higher at low shear rates and thins as the admixture viscosity approaches the pure suspension viscosity at high shear rates. At high shear rates, the curves both with and without added water approach each other and the theoretical value for pure suspensions. At these high shear rates, capillary structures cannot form and the secondary fluid content does not influence the viscosity of the suspensions. The shape of these curves appears to depend on the particle size with the viscosity of larger particles decreasing more rapidly than for smaller particles. The capillary suspension for the smallest particles ( $r = 1.19$   $\mu\text{m}$ ) drops rapidly above a shear rate of 100 s $^{-1}$ , likely due to slip.

The variation of the capillary suspension viscosity on the particle radius at a single shear rate (50 s $^{-1}$ ) is shown in Fig. 7b. Although the effect of the capillary forces on the suspension rheology is much less pronounced, the dependence on the reciprocal particle radius persists even at this higher shear rate. This suspension without added fluid is virtually independent of the particle size (for all but the smallest particles) indicating the disintegration of clusters formed by the weaker van der Waals

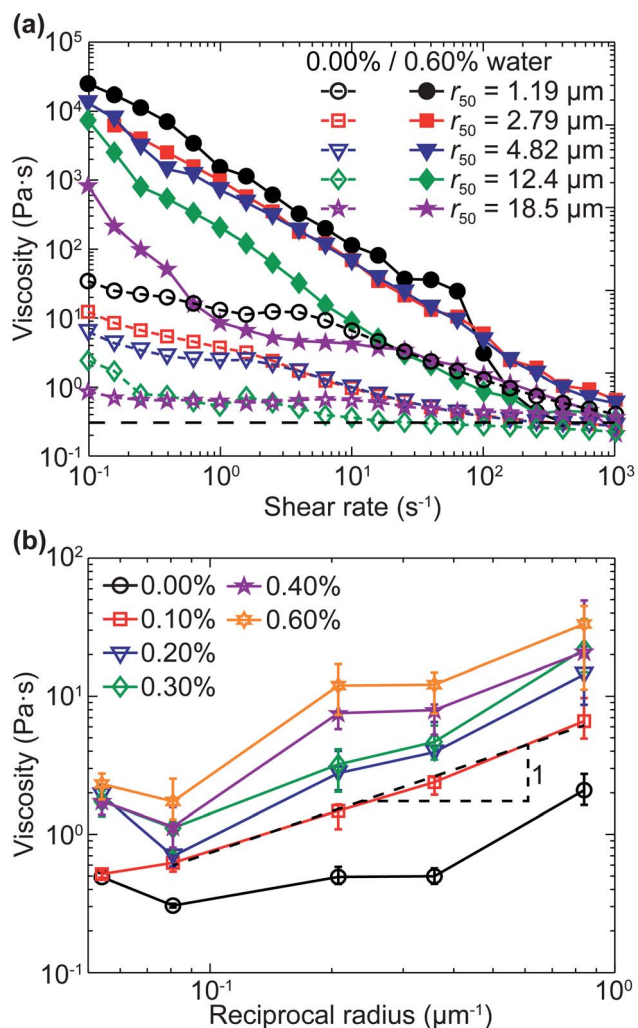


**Fig. 7** (a) Flow curves for various particle sizes both without and with 0.60% added water. The lower dashed line gives the effective viscosity for a concentrated suspension using the relation of Quemada<sup>39</sup> where  $\phi_m = 0.6$ . (b) Viscosity at  $50 \text{ s}^{-1}$  as a function of the particle reciprocal radius in the pendular state. (Clean glass,  $\phi = 0.30$ , in DINP with added water, pendular state.)

attraction. For the mixtures with added water, particles agglomerated from a capillary force will break up as the shear rate increases, but the size and strength of these agglomerates varies with the particle size indicating the presence of capillary attraction even at this higher shear rate. There exists a critical particle separation for capillary bridges having a specified secondary fluid volume at which the bridge will break.<sup>14</sup> The particle size should not change this separation, but the force exerted on the particles at the time of break up will vary according to the particle size. There may also be some influence on the rate of bridge formation and destruction that depends on the particle size. The viscosity is independent of the particle radius at high shear rates due to the complete destruction of the capillary network.

Also shown in these diagrams (Fig. 6 and 7b) is the dependence on the addition of a secondary fluid. The difference in both the yield stress and viscosity between the mixtures without added water and with 0.1% wt. added water is greater than between

0.1% and 0.2%. For the larger fractions of water, there appears to be a plateau or decreasing dependence of the resultant behavior on secondary fluid content. This rapid increase followed by a plateau is characteristic of capillary suspensions.<sup>1,9</sup>

### Surfactants

The addition of surfactants to a capillary suspension reduces the interfacial tension between the two fluids, thereby reducing the strength of the suspension. This affect is investigated using admixtures of hydrophobic calcium carbonate suspended in silicone oil (AK200,  $\phi = 0.13$ ) with added water (capillary state,  $\theta = 139.2^\circ$ ). The interfacial tension decreases from  $39.8 \text{ mN m}^{-1}$  without surfactant to  $5.7 \text{ mN m}^{-1}$  with small amounts of nonionic surfactants for the silicone oil and water interface used in this experiment. The CMC for these surfactants is very low and all the surfactant concentrations tested below are above the CMC, such that additional surfactant concentration results in very little change to the interfacial tension.

In addition, the surfactants change the contact angle between the solid particles and the two fluids. The contact angle that the water makes against the calcium carbonate particles in a silicone oil environment without surfactant is  $139.2^\circ$ . With surfactant, this contact angle has a value near  $180^\circ$  and can not be calculated from the contact angles measured in air. This change, in particular, can make the formation of a capillary network feasible or impossible. Three different nonionic surfactants with varying HLB were tested in capillary state suspensions. The surfactants were added to the bulk fluid (silicone oil) at the same time as the secondary fluid and mixed thoroughly. The surfactant will be present at the interface between the two fluids, attached to the solid particles, and (as we are above the CMC) form micelles within the bulk phase.

The addition of small amounts of surfactants, as demonstrated in Fig. 8, increases the yield stress for suspensions without added water. The surfactant decreases agglomeration of the  $\text{CaCO}_3$  particles within the oil phase, further strengthening the van der

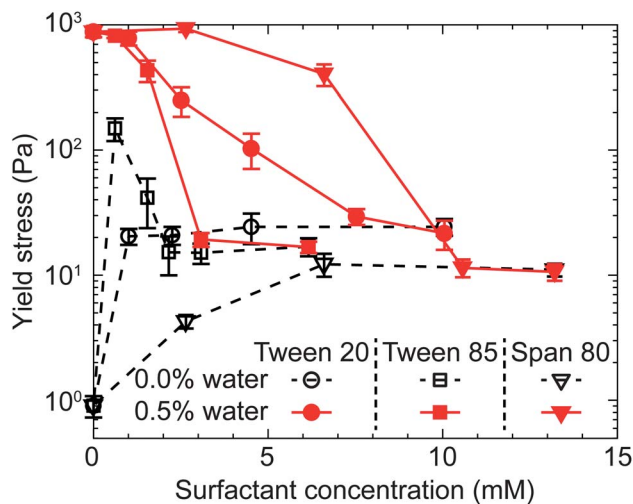


**Fig. 8** Influence of the surfactant concentration on yield stress for all of the nonionic surfactants tested (Tween 20: HLB = 16.7, Tween 85: HLB = 11.0, Span 80: HLB = 4.3). (Hydrophobic calcium carbonate,  $r = 0.79 \text{ } \mu\text{m}$ , in silicone oil,  $\phi = 0.13$ , with added water, capillary state.)

Waals network. The exact influence of the surfactant concentration on suspensions without added water varies by surfactant type.

The yield stress for the sample with 0.5% added water decreases towards a limiting value matching the yield stress of the suspension without added water as the surfactant concentration is increased. This behavior appears to be typical of nonionic surfactants and is demonstrated in all the surfactants tested. The concentration of surfactant necessary to reach the limit value varies with the surfactant type and appears to show no correlation with the HLB. The observed reduction in yield stress is much greater than the change in interfacial tension, demonstrating that with increasing surfactant concentration the number of capillary interaction sites must also be reduced. Similar results were obtained for suspensions with 0.2% added water, but in this case the amount of surfactant needed to apparently destroy the capillary force network was reduced (data not shown).

For the capillary state suspension including 0.5% water (Fig. 8) the yield stress decreases by two orders of magnitude with added surfactant. This reduction is much greater than the decrease of the interfacial tension (between  $39.8 \text{ mN m}^{-1}$  and  $5.7 \text{ mN m}^{-1}$ , a reduction of less than an order magnitude). This leaves the influence of the surfactant concentration on the contact angle as the cause of the observed decrease in the strength. This contact angle was calculated using the Young equation (eqn (4)) and increases from  $139.2^\circ$  without added surfactant to a calculated value of  $180^\circ$  with small amounts of added surfactant. Calculating the two-fluid contact angle from the contact angle measurements in air at these high contact angles does not yield an exact value of the actual contact angle,<sup>40</sup> but the contact angle is significantly higher with the added surfactant than without.

As was shown in a previous article, capillary state suspensions are formed from networked subgroupings of particles surrounding secondary fluid droplets.<sup>9</sup> These particle subgroupings can arrange in tetrahedral, octahedral, or higher order structures depending on the secondary fluid content and the contact angle that the secondary fluid makes with the solid particles. When the contact angle becomes high, certain particle arrangements become inaccessible (*e.g.* greater than  $151.2^\circ$  for tetrahedral and  $165.3^\circ$  for octahedral structures).<sup>9</sup> Without these structures, which would otherwise form a strong capillary network at low water content, the weaker vdW network becomes the sole contribution to the formation of a sample-spanning network in these samples. The reduction in the yield stress of the samples with added water towards the values without added water at high surfactant concentrations implies that the presence of the secondary fluid is no longer important—a situation that would occur if the contact angle increases beyond the critical contact angle making the creation of capillary suspensions impossible. The surfactants also stabilize the water droplets making the detachment of these droplets from the particles more energetically favorable.

To confirm the increase in the contact angle with added surfactant and its influence on the particle–secondary fluid structures, a similar system using glass beads that were hydrophobically modified was imaged using light microscopy (Fig. 9). The particles were suspended in silicone oil (AK200) with 1% added water (without surfactant,  $\theta = 99.3^\circ$ ) and 0.5% nonionic surfactant Span 80 (10.6 mM). The admixture was created at

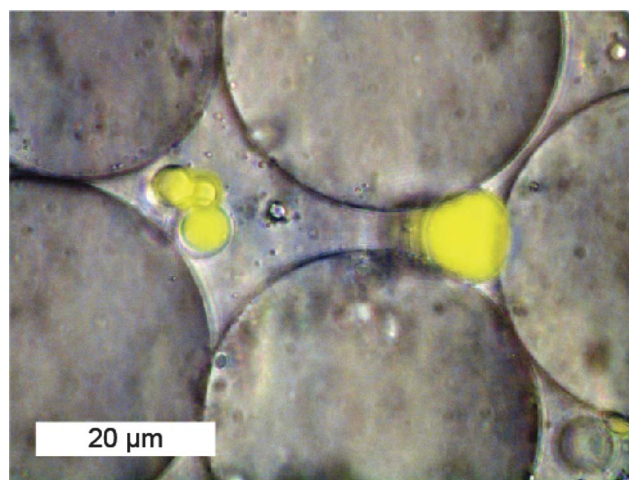


**Fig. 9** Image of a capillary suspension with added surfactant Span 80 (droplet locations, determined from the fluorescent image, are colored yellow). The larger drop on the right is still attached to three particles ( $\theta = 130^\circ$ ) and the droplet grouping on the left is unattached. (Hydrophobically modified glass,  $r = 18.5 \mu\text{m}$ , in silicone oil,  $\phi = 0.40$ , with 1% added water, capillary state. Without surfactant,  $\theta = 99.3^\circ$ .)

$\phi = 0.40$  and diluted in additional silicone oil before imaging. The fluorescent dye (PromoFluor-488 Premium, carboxylic acid) was added to the water to aid in locating the secondary fluid droplets.

In Fig. 9, a water droplet can be seen on the right still attached to three particles. This droplet makes an average contact angle of  $\theta = 130^\circ$ , significantly higher than the contact angle of  $99.3^\circ$  without surfactant. On the left, three droplets are visible. Obviously, the surfactant completely surrounds these droplets, stabilizing them from coalescing into a larger droplet and increasing the contact angle such that they detach from the particles. These droplets will not contribute to the formation of a strong sample-spanning network as does the droplet on the right where the stronger capillary force is existent. As with the imaged glass capillary suspension, the influence of the added surfactant on the calcium carbonate admixtures should result in the detachment of droplets from the particle subgroupings. This reduction in the number of capillary subgroupings with increasing surfactant concentration should significantly reduce the strength of the sample-spanning network and, with sufficient surfactant concentration, completely prevent the subgroupings from being formed. At this high surfactant concentration, there should be no discernible difference between the strength of the admixtures with and without secondary liquid, the exact situation shown in Fig. 8.

Similar effects were achieved by adding the more hydrophilic surfactant docusate sodium (DOSS) to the water phase. These experiments mirror the measurements with the non-ionic surfactants, where the addition of a surfactant results in a reduction of the yield stress, but a higher molar concentration of the ionic surfactant was required. The effect of two surfactants, the ionic surfactant DOSS added to the water phase and the nonionic surfactant Tween 85 added to the oil phase, on the yield stress reduces the yield stress more than with the nonionic surfactant alone. This reduction retains the shape of the yield

stress curve, but shifts it to the left (lower Tween 85 concentrations).

## Conclusions

Capillary suspensions, suspensions with the addition of small amounts of a secondary immiscible fluid, form a new class of materials. Capillary forces can be used to form strong particle networks, which can be used as precursors for the manufacture of porous solids or membranes. Moreover, the mechanical features of these suspensions can be varied in a wide range to meet the specific needs of a particular processing step or application technique. This current work investigates several methods to modify the rheological properties through the choice of particle size, the addition of surfactants, or through the variation of the sample temperature.

The intensity of the capillary stress is proportional to the reciprocal particle radius implying that decreasing the particle size would result in the strengthening of capillary suspensions. This relationship was demonstrated for samples in the pendular state (where the secondary fluid preferentially wets the particles) for particles with radii between 1 and 20  $\mu\text{m}$ . There was a change in the yield stress of approximately one order of magnitude between the stronger network formed by the smaller (1  $\mu\text{m}$ ) particles and the weaker network formed using the larger (20  $\mu\text{m}$ ) particles. For the larger particles, the pure suspension was unstable and would rapidly phase separate, but with the addition of less than 0.5% secondary fluid, these suspensions formed sample-spanning networks and were stable for very long periods of time (>1 week). The low shear viscosity of such admixtures showed a similar dependence on the particle radius as well as the strong shear thinning. At high enough shear rates, the network is destroyed and the viscosity is independent of particle size as expected. The larger particles were more sensitive to the applied shear field with the viscosity decreasing more rapidly and at lower shear rates.

Adjusting the sample temperature is also able to modify the admixture strength by approximately one order of magnitude over a 50 °C temperature range for the calcium carbonate particles in the capillary state. The magnitude of the capillary force is proportional to the interfacial tension between the two fluids such that decreasing the interfacial tension by increasing the sample temperature will decrease the strength of the capillary suspension. Through the evaporation of the secondary fluid, these capillary suspensions return to the state of the pure suspension, decreasing the yield stress and viscosity by several orders of magnitude. The process of adding and subsequently removing the secondary fluid can be repeated without any sample degradation. The ability to adjust the properties of these suspensions through the external factor of sample temperature is particularly advantageous to many industrial processes.

Finally, this current work investigated the use of surfactants to adjust the strength of the capillary suspensions. Surfactants are able to modify the interfacial tension between the two liquids as well as the contact angle that the secondary fluid makes with the solid particles when surrounded by the bulk fluid. Capillary state suspensions are particularly sensitive to changing contact angles and have a limited range where the formation of a network is possible. With the addition of surfactants, the yield stress was

reduced by two orders of magnitude as the number of capillary bridges was decreased. The rate of this reduction, as a function of surfactant concentration, depends on the surfactant type. All of the nonionic surfactants tested show no difference between the pure suspensions and the suspensions with added water for surfactant concentrations greater than 15 mM. The addition of an ionic surfactant to the secondary fluid was also able to reduce the yield stress alone and in cooperation with a nonionic surfactant added to the bulk fluid.

All three methods of adjusting the strength of capillary suspensions explored in this paper can be used separately or in coordination to modify the strength of these suspensions to varying degrees. One's ability to modify these capillary suspensions makes them particularly well suited for various industrial processes and they may be an inexpensive alternative to other fluids and suspensions that possess tunable properties. In addition to industrial processes, this work may be important in understanding the influence of trapped air bubbles in suspensions<sup>41</sup> and how the influence of these air bubbles may be mitigated.

## Acknowledgements

We are grateful to the German Research Foundation (Deutsche Forschungsgemeinschaft grant no. WI3138/6-1) for financial support. We are also appreciative of a referee for drawing our attention to the problem of air bubbles trapped in suspensions.

## Notes and references

- 1 E. Koos and N. Willenbacher, *Science*, 2011, **331**, 897–900.
- 2 E. Koos, J. Dittmann and N. Willenbacher, *Chem. Ing. Tech.*, 2011, **83**, 1305–1309.
- 3 S. V. Kao, L. E. Nielsen and C. T. Hill, *J. Colloid Interface Sci.*, 1975, **53**, 367–373.
- 4 C. Gögelein, M. Brinkmann, M. Schröter and S. Herminghaus, *Langmuir*, 2010, **26**, 17184–17189.
- 5 K. Cavalier and F. Larché, *Colloids Surf., A*, 2002, **197**, 173–181.
- 6 J. P. K. Seville, C. D. Willett and P. C. Knight, *Powder Technol.*, 2000, **113**, 261–268.
- 7 J. Dittmann, E. Koos, N. Willenbacher and B. Hochstein, *Verfahren zur Herstellung einer porösen Keramik und damit erhältliche poröse Keramik*, German Patent, DE 10 2011 106 834.5, 2011.
- 8 J. McCulfor, P. Himes and M. R. Anklam, *AIChE J.*, 2010, 12451.
- 9 E. Koos and N. Willenbacher, *Soft Matter*, 2012, **8**, 3988–3994.
- 10 V. P. Mehrotra and V. S. Sastry, *Powder Technol.*, 1980, **25**, 203–214.
- 11 F. M. Orr, L. E. Scriven and A. P. Rivas, *J. Fluid Mech.*, 1975, **67**, 723–742.
- 12 C. Gao, *Appl. Phys. Lett.*, 1997, **71**, 1801–1803.
- 13 C. D. Willett, M. J. Adams, S. A. Johnson and J. P. K. Seville, *Langmuir*, 2000, **16**, 9396–9405.
- 14 G. Lian, C. Thornton and M. J. Adams, *J. Colloid Interface Sci.*, 1993, **161**, 138–147.
- 15 H. J. Butt, *Langmuir*, 2008, **24**, 4715–4721.
- 16 D. Megias-Alguacil and L. J. Gauckler, *AIChE J.*, 2009, **55**, 1103–1109.
- 17 H. J. Butt and M. Kappl, *Adv. Colloid Interface Sci.*, 2009, **146**, 48–60.
- 18 H. Schubert, *Powder Technol.*, 1984, **37**, 105–116.
- 19 W. B. Pietsch and H. Rumpf, *Chem. Ing. Tech.*, 1967, **39**, 885–893.
- 20 H. Rumpf, *Agglomeration*, Interscience, John Wiley & Sons, New York, 1962, pp. 379–418.
- 21 H. Schubert, *Kapillarität in porösen Feststoffsystemen*, Springer-Verlag, Berlin, 1982.
- 22 G. Gillies, K. Büscher, M. Preuss, M. Kappl, H. J. Butt and K. Graf, *J. Phys.: Condens. Matter*, 2005, **17**, S445–464.
- 23 S. Stiller, H. Gers-Barlag, M. Lergenmueller, F. Pflücker, J. Schulzb, K. P. Wittern and R. Daniels, *Colloids Surf., A*, 2004, **232**, 261–267.



- 24 L. Yan, K. Wang, J. Wu and L. Ye, *Colloids Surf. A*, 2007, **296**, 123–131.
- 25 R. N. Wenzel, *Ind. Eng. Chem.*, 1936, **28**, 988–994.
- 26 H. Nakae, R. Inui, Y. Hirata and H. Saito, *Acta Mater.*, 1998, **46**, 2313–2318.
- 27 C. O. Fournier, L. Fradette and P. A. Tanguy, *Chem. Eng. Res. Des.*, 2009, **87**, 499–506.
- 28 R. Aveyard, B. P. Binks and J. H. Clint, *Adv. Colloid Interface Sci.*, 2003, **100–102**, 503–546.
- 29 Experiments show that the yield stress does not change if the surfactant is added to the suspension prior to adding the secondary fluid, added at the same time as the secondary fluid, or added to the capillary suspension after the addition of the secondary fluid.
- 30 L. L. Schramm, *Emulsions, Foams and Suspensions: Fundamentals and Applications*, Wiley-VCH, Weinheim, Germany, 2005.
- 31 P. M. Kruglyakov, *Hydrophile–lipophile balance of surfactants and solid particles: Physicochemical aspects and applications*, Elsevier Science, Amsterdam, 2000.
- 32 The rate of change in stress  $\Delta \log \sigma / \Delta t$  was always greater than  $0.25\% \text{ s}^{-1}$ . Ramp times shorter than 10 min ( $\Delta \log \sigma / \Delta t > 0.5\% \text{ s}^{-1}$ ) resulted in a significant error between samples.
- 33 D. Villers and J. K. Platten, *J. Phys. Chem.*, 1988, **92**, 4023–4024.
- 34 H. Inaba and K. Sato, *Fluid Phase Equilib.*, 1996, **125**, 159–168.
- 35 H. Matsubara, M. Murase, Y. H. Mori and A. Nagashima, *Int. J. Thermophys.*, 1998, **9**, 409–424.
- 36 This mixture is in the capillary state where  $\cos\theta < 0$ . As we are interested in the strength of these mixtures and the  $\cos\theta$  is used as a predictive value only, we take the magnitude of this value.
- 37 G. K. Batchelor, *J. Fluid Mech.*, 1977, **83**, 97–117.
- 38 H. A. Barnes, *J. Rheol.*, 1989, **33**, 329–366.
- 39 D. Quemada, *Rheol. Acta*, 1977, **16**, 82–94.
- 40 B. P. Binks and J. H. Clint, *Langmuir*, 2002, **18**, 1270–1273.
- 41 E. Brown, H. Zhang, N. A. Forman, B. W. Maynor, D. E. Betts, J. M. De Simone and H. M. Jaeger, *Phys. Rev. E: Stat., Nonlinear, Soft Matter Phys.*, 2011, **84**, 031408.

---

## Addition and correction

---

[View Online](#)

### Note from RSC Publishing

This article was originally published with incorrect page numbers. This is the corrected, final version.

---

The Royal Society of Chemistry apologises for these errors and any consequent inconvenience to authors and readers.

---